

# Low-Profile Wideband Circularly Polarized Metasurface Antenna for 5G Application

Manoj N N

*Dept. of Electronics and Telecommunication Engineering  
Siddaganga Institute of Technology  
Tumkuru, India  
manoj.1si23et408@gmail.com*

Rohith H C

*Dept. of Electronics and Telecommunication Engineering  
Siddaganga Institute of Technology  
Tumkuru, India  
rohith.1si22et045@gmail.com*

Manoj U H

*Dept. of Electronics and Telecommunication Engineering  
Siddaganga Institute of Technology  
Tumkuru, India  
Manoj.1si22et015@gmail.com*

Rakshith K

*Dept. of Electronics and Telecommunication Engineering  
Siddaganga Institute of Technology  
Tumkuru, India  
rakshith.1si23et414@gmail.com*

Puneeth Kumar Tharehalli Rajanna

*Dept. of Electronics and Telecommunication Engineering  
Siddaganga Institute of Technology  
Tumkuru, India  
punithkumartr@sit.ac.in*

**Abstract**—In this paper, a low profile circularly polarized single layer metasurface based antenna is designed and validated through simulation. The antenna consists of non-uniform metasurface on the front side of the substrate and a co-planar waveguide(CPW) fed slot antenna on the back side. The slot is oriented at  $45^0$  with respect to xy plane. The metasurface consists of two different sized unit cells to obtain two resonant modes. The each unit cell is rectangular shaped where its dimensions are adjusted to achieve orthogonal phase shift required to obtain circular polarization. The larger dimension center patches are responsible for lower resonant frequency and smaller patches surrounded which are place in the corner are responsible for obtaining higher resonance frequency. The two resonances are combine to achieve wider axial ratio bandwidth. The simulated impedance bandwidth of 55.01% and an ARBW of 12.58% is obtained. The peak gain of 7.92dBi is achieved at 5.75GHz with 0.5dBi variation over the entire bandwidth. The radiation pattern is oriented in broadside direction with better cross-polarization value of minimum -20dB in both XZ and YZ plane. The results demonstrates that this design is well suitable for modern 5G communication which demands the consistent gain, good polarization purity and wide bandwidth.

**Index Terms**—Circularly polarized antenna, metasurface, axial-ratio bandwidth, Low profile, Unit cell.

## I. INTRODUCTION

Nowadays the wireless communication standards such 5G is extensive grown up to reach the requirement of modern era which needs high data rate, wider bandwidth, good resolution, high gain and long distance communication. In this regard, the antenna designs plays a very crucial role to meet the requirements of 5G. conventional antennas suffers a lot from compactness, antenna profile, wider bandwidth, polarization

purity, high gain and many more. to mitigate the above issues, metasurfaces are the potential solution. The dual band monopole antenna is designed in [1] requires a complex feeding network and has less impedance matching over wide bandwidth. A compact via-free metasurface-based monopole antenna for dual-band dual-polarized operation is aimed at off-body communication systems in [2].The study illustrated how metasurface integration can improve polarization properties while keeping a small footprint. The implementation of systematic mode-based analysis represented a dramatic shift in CP antenna design. In [3], Characteristic Mode Analysis (CMA) is used to create a broadband single-layer metasurface antenna. The antenna increased its impedance bandwidth, axial-ratio bandwidth, and radiation efficiency by selectively activating orthogonal characteristic modes. This study demonstrated the usefulness of CMA as a design tool for broadband CP metasurface antennas. Wideband performance, metasurface engineering, MIMO capabilities, and adaptable implementations are used in [4-6]. A wideband two-element CP MIMO antenna with excellent isolation and polarization diversity, which results in reduced envelope correlation and increased MIMO performance [4]. The article [5] shown that metasurface-loaded CP antennas can increase axial-ratio bandwidth while decreasing radar cross section without increasing antenna thickness. An inkjet-printed flexible dual-band dual-sense CP patch antenna was also demonstrated, demonstrating advances in low-cost fabrication and wearable antenna applications [6]. Recent research in 2025 focuses on multimode excitation, functional integration, and intelligent optimization. [7] describes an integrated low-RCS CP antenna based on a

multimode metasurface that improves bandwidth by controlling the excitation of several resonant modes. A wideband CP filtering metasurface antenna with split-ring resonators and parasitic patches, resulting in increased bandwidth and inherent filtering properties [8]. Also presented is an inverse antenna design process based on generative artificial intelligence, demonstrating the potential of AI-driven optimization for the rapid synthesis of high-performance antenna designs [9]. Metasurface-assisted antennas have emerged as a viable option for enhancing bandwidth, gain, and polarization purity without adding structural complexity. However, many present CP designs are based on multilayer typologies, elaborate unit-cell geometries, or sophisticated perturbation mechanisms, which limit fabrication aspect and axial-ratio bandwidth. To overcome these issues, this paper introduces a single-layer wideband CP metasurface antenna designed for the Sub-6 GHz 5G range.

## II. ANTENNA DESIGN AND MECHANISM

### A. Antenna Structure

Figure 1 shows the structure of the proposed metasurface-based antenna. The antenna is made up of varying size rectangular-shaped unit cells on the front side of the substrate material. The backside of the substrate utilizes a slot-based stimulation technique. The CPW feed is utilized with slots inclined  $45^\circ$  with respect to the XY plane. The optimized

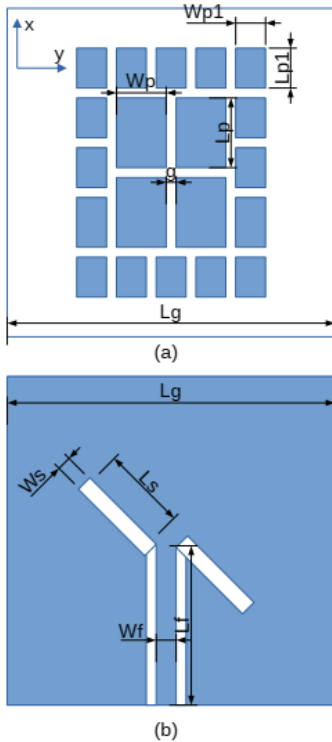


Fig. 1. (a) non-uniform Metasurface (front view) (b) feeding mechanism using CPW technique (Back view).

dimensions of the proposed metasurface-based circularly polarized antenna are listed as follows:  $l_g = 70$  mm,  $l_p = 13$  mm,

$l_p s = 12.8$  mm,  $l_l = 12$  mm,  $w_p = 9.8$  mm,  $w_p s = 9.4$  mm,  $h_s = 3.2$  mm,  $s_1 = 1.05$  mm,  $w_f = 1$  mm,  $w_{f1} = 1$  mm,  $s = 0.70$  mm,  $h_s = 0.70$  mm,  $w_{p1} = 0.65$  mm,  $g = 0.5$  mm,  $g_f = 0.2$  mm,  $g_1 = 0.16$  mm, and  $t = 0.035$  mm. The metasurface is intended to improve circular polarization performance by modifying the wavefront and increasing axial-ratio bandwidth while keeping a small footprint. Figure 1b shows the antenna's back perspective, with the radiating layer constructed on an RT5880 substrate and activated by a slanted slot feed arrangement. The feed geometry introduces the necessary perturbation to excite two orthogonal field components, allowing circular polarization to be generated when paired with the metasurface's designed surface currents. The location of the radiating element right behind the metasurface results in strong coupling between the two layers, which increases impedance matching, gain, and bandwidth. Fig. 2 depicts the 3D far-field distribution of the proposed metasurface antenna. This small design uses the metasurface to generate wideband circular polarization without the need for sophisticated multilayer stacks or extensive feeding networks, making the antenna ideal for Sub-6 GHz 5G applications that require high efficiency, wide bandwidth, and structural simplicity.

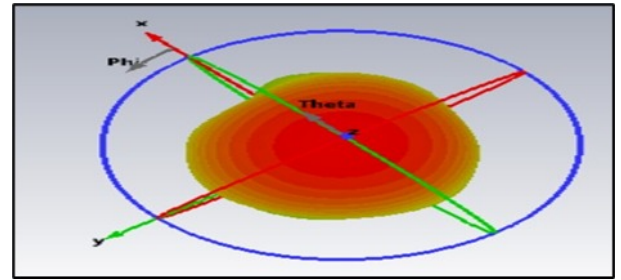


Fig. 2. Simulated results of the antenna 3D radiation pattern

### B. Antenna Working Mechanism

The proposed metasurface antenna operates through the excitation and interaction of two resonant modes formed by the  $3 \times 4$  array of sub-wavelength rectangular patches printed on the RT5880 substrate. The CPW fed slot oriented  $45^\circ$  with respect to xy plane excites the metasurface. The slot is linearly polarized which splits the E field components into x and y directed fields. These  $E_x$  and  $E_y$  components imposed on to the metasurface which creates the surface currents on two different sized unit cells via inductive and capacitive coupling. Since the unit cells of different sizes are in close proximity, the surface current extends to till corner patches. The center patches which are larger in size is designed to obtain lower frequency resonant mode and corner smaller size patches are designed to achieve higher frequency resonant mode. The two resonant modes are combined together to achieve wide bandwidth. By carefully tuning the unit cell dimensions, the stable  $90^\circ$  phase shift across a broad frequency range is obtained. Consequently, the surface currents exhibit a rotational behavior with time, converting the initial coplanar waveguide (CPW) excitation into a circularly polarized (CP) radiated

wavefront. At lower frequencies, the current density is mainly concentrated on the center patches. As the frequency increases, the energy gradually shifts toward the corner patches. This dynamic redistribution of energy strengthens the orthogonal field components and helps maintain a stable phase difference. Ultimately, the metasurface acts as a sophisticated phase-transforming layer, converting a standard linear feed into the wideband, high-purity CP radiation required for sub-6 GHz 5G application.

### C. PARAMETRIC STUDY

The parametric analysis was performed to determine how modifications in geometry of the antenna and feeding parameters affect the antenna's impedance and axial ratio performance. The proposed antenna is primarily based on electromagnetic coupling between the metasurface patches and the orientation of the CPW feed, even little modification to these parameters have a significant impact on resonance behavior, circular-polarization performance, and radiation stability. Among the parameters investigated, the dimensions of centered metasurface patches were critical because they are responsible for the lower-frequency resonance and by increasing their size shifts the fundamental resonance to lower frequency and can improve impedance matching but may degrade axial-ratio performance, whereas decreasing their size pushes the resonance higher frequency and reduces coupling with the outer patches, thereby narrowing the circular-polarization bandwidth. The CPW feed's orientation angle ( $45^\circ$ ) considerably affected the excitation balance of orthogonal modes. An exact angle produces the good axial ratio value, but deviations caused axial-ratio value degradation, reduced axial ratio bandwidth and increases cross-polarization levels. Thicker substrates boosted gain by widening the effective aperture but could introduce surface waves, while differences in dielectric constant altered resonance frequencies by changing the guided wavelength. Overall, the parametric analysis determined the best combination of patch dimensions, inter-element spacing, feed orientation, and substrate properties for achieving a wide impedance bandwidth, low axial ratio, high radiation efficiency, and stable broadside radiation. The analysis indicates that the antenna's performance is very sensitive to these factors. Precise adjustment is done to accomplish the needed wideband circular polarization for Sub-6-GHz-5G applications.

### III. RESULTS AND DISCUSSION

The performance of the proposed metasurface antenna was thoroughly evaluated. Full-wave simulations using CST Microwave Studio were used to analyze the antenna's characteristics, with an emphasis on impedance behavior, axial-ratio response, radiation patterns, gain, and efficiency. The simulated  $S_{11}$  profile demonstrates excellent impedance matching, achieving  $|S_{11}| < -10$  dB across a wide frequency range, indicating effective power transfer from the CPW feed to the metasurface and confirming the presence of multiple closely spaced resonances generated by the interaction of

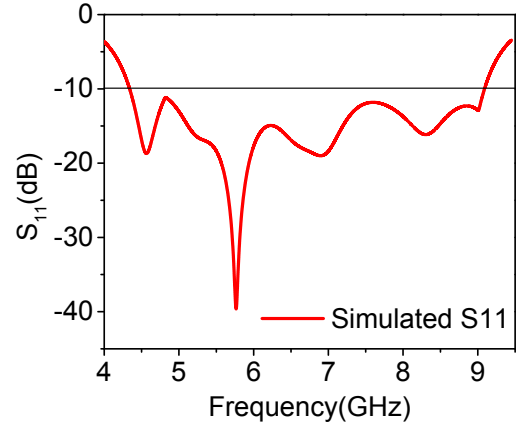


Fig. 3. Simulated reflection coefficient in dB( $S_{11}$ )

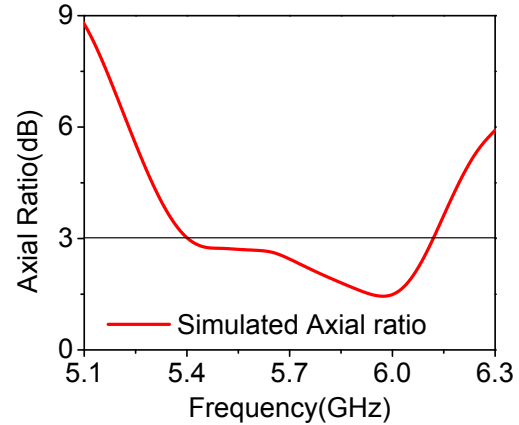


Fig. 4. Simulated axial ratio in dB

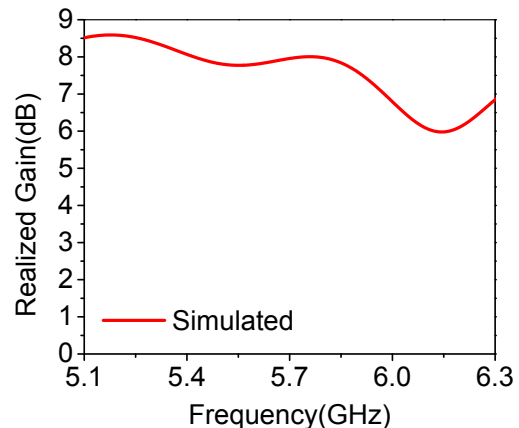


Fig. 5. Simulated gain plot in dB

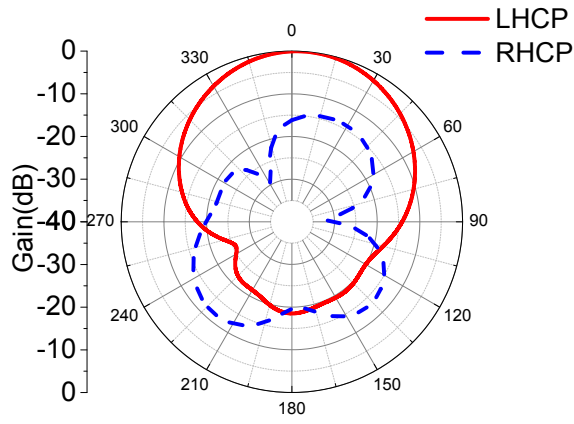


Fig. 6. Simulated radiation pattern of proposed design at 5.5GHz in XZ plane

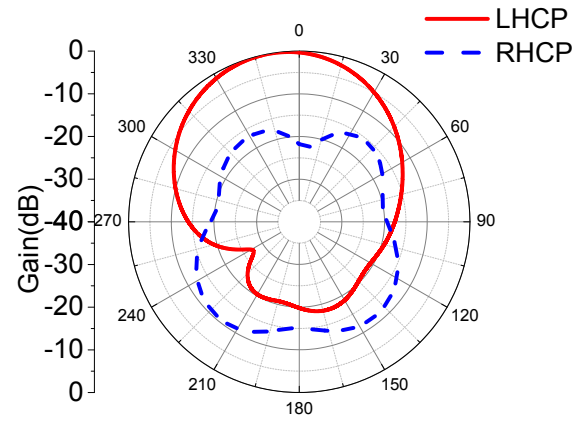


Fig. 8. Simulated radiation pattern of proposed design at 5.94GHz in XZ plane

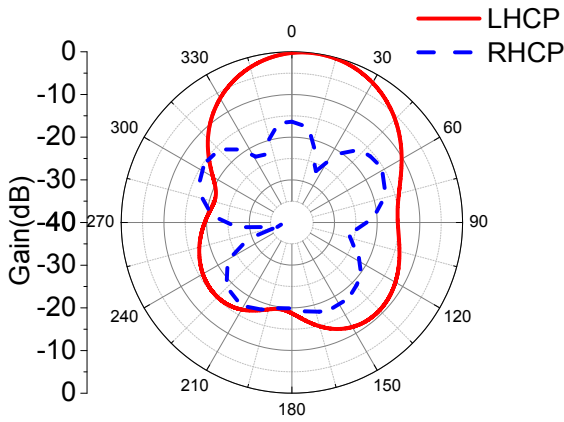


Fig. 7. Simulated radiation pattern of proposed design at 5.5GHz in YZ plane

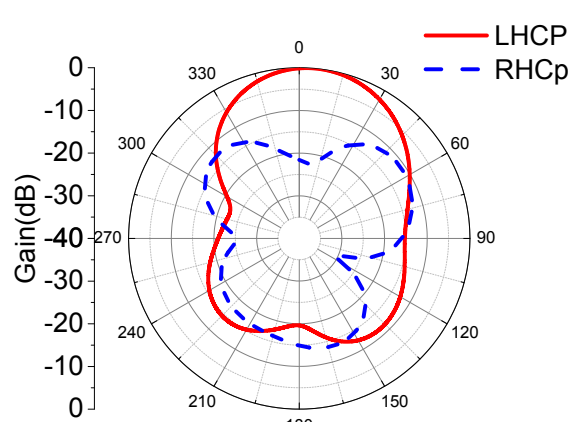


Fig. 9. Simulated radiation pattern of proposed design at 5.94GHz in YZ plane

central and corner patches. This multi-resonant activity broadens the impedance bandwidth and allows for the stimulation of orthogonal modes necessary for circular polarization. The antenna maintains  $AR < 3$  dB across a significant portion of the working band, indicating dependable circular-polarization performance. The  $3 \times 4$  metasurface array and tilted CPW feed provide a wide AR bandwidth. The impedance bandwidth runs from 5.56GHz to 9.78GHz (55.01%), with an axial ratio bandwidth of 5.39GHz-6.11GHz (12.58%). Figures 3 and 4 provide simulated impedance and axial ratio bandwidth graphs. The simulated gain is around 7.2 dBi, with a directivity of 7.6 dBi. This results in a radiation efficiency of approximately 91%, demonstrating the metasurface's low loss and effectiveness. The simulated gain plot is given in Figure 5. Radiation-pattern analysis at several frequencies across the band demonstrates that the antenna consistently generates broadside radiation with a well-formed main lobe and low distortion. The co-polarized component remains dominating, while cross-polarized fields are greatly reduced, indicating strong polarization purity. At 5.5GHz, 5.94GHz, and 6.11GHz,

the patterns remain symmetrical with low sidelobe levels, demonstrating stable far-field behavior over the entire bandwidth. The 3D radiation plots further show that the antenna maintains a uniform and smooth beam shape with energy concentrated effectively in the broadside direction. The radiation pattern At 5.5GHz, 5.94GHz, and 6.11GHz, the patterns are symmetrical with low sidelobe levels, indicating steady far-field behavior across the full bandwidth. The 3D radiation plots further reveal that the antenna has a homogeneous and smooth beam shape, with energy concentrated effectively in the broadside direction. Figures 6, 7, 8, and 9 illustrate the radiation patterns at 5.5GHz and 5.94GHz. Furthermore, the antenna exhibits low cross-polarization levels (ranging from  $-15.5$  dB to  $-22.3$  dB across different frequencies), confirming the mode purity needed for reliable CP operation. Overall, the results confirm that the proposed antenna achieves wide impedance bandwidth, broad axial-ratio bandwidth, high gain, low cross-polarization, and stable radiation patterns, demonstrating its strong potential for integration in compact, low-profile, and

high-efficiency Sub-6-GHz 5G communication platforms.

#### IV. CONCLUSION

This paper introduces a single-layer  $3 \times 4$  metasurface antenna designed for broadband circular polarization in Sub-6-GHz 5G communication systems. The design achieves the required  $90^\circ$  phase quadrature for high-purity RHCP/LHCP radiation by integrating rectangular patches on a Rogers RT5880 substrate with an angled CPW feed. The antenna achieves a peak gain of  $7.2\text{dBi}$  and a high radiation efficiency of 91% through improved modal hybridization and aperture usage. The performance results confirm good impedance matching ( $|S_{11}| < -10\text{dB}$ ) is 55.01% and a steady axial ratio  $AR < 3\text{dB}$  is 12.58% throughout a significantly widened bandwidth. The symmetrical broadside patterns and excellent cross-polarization suppression (up to  $-22.3\text{dB}$ ) provide dependable far-field features for high-capacity wireless networks. This compact, low-profile architecture offers a high-performance radiating solution perfectly suited for integration into portable 5G platforms, drones, and IoT devices.

#### ACKNOWLEDGEMENT

The authors would like to acknowledge the support provided by the **5G Use Cases Laboratory** for facilitating this research work. The infrastructure, technical resources, and facilities available in the 5G Use Cases Lab significantly contributed to the successful completion of this study. The authors sincerely thank the laboratory team for their valuable support and assistance during the course of this work.

#### REFERENCES

- [1] A. Bhattacharjee and S. Dwari, "A monopole antenna with reconfigurable circular polarization and pattern tilting ability in two switchable wide frequency bands," *IEEE Antennas Wireless Propag. Lett.*, vol. 20, no. 9, pp. 1661–1665, Sep. 2021.
- [2] N. K. Sahu and S. K. Mishra, "Compact dual-band dual-polarized monopole antennas using via-free metasurface for off-body communications," *IEEE Antennas Wireless Propag. Lett.*, vol. 21, no. 7, pp. 1358–1362, Jul. 2022.
- [3] A. El Yousif, A. Lamkaddem, K. A. Abdalmalak, and D. Segovia-Vargas, "A broadband circularly-polarized single-layer metasurface antenna using characteristic mode analysis," *IEEE Trans. Antennas Propag.*, vol. 71, no. 4, pp. 1231–1245, Apr. 2023, doi: 10.1109/TAP.2023.3239104.
- [4] Z. M. Phyo, T. Fujimoto, and C.-E. Guan, "Wideband circularly polarized two-element MIMO antenna with polarization diversity," *IEICE Commun. Express*, vol. 13, no. 12, pp. 487–491, Dec. 2024, doi: 10.23919/comex.2024COL0021.
- [5] X. Zhang, Q. Chen, W. Geng, and Q. Guo, "A wideband circularly polarized meta-antenna with low radar cross section," *IEEE Antennas Wireless Propag. Lett.*, vol. 23, no. 12, pp. 4643–4646, Dec. 2024, doi: 10.1109/LAWP.2024.3463171.
- [6] A. R. Hossain, M. S. I. Sagar, A. A. Marty, P. K. Sekhar, and T. Karacolak, "Inkjet printer flexible dual-band dual-sense circularly polarized patch antenna," *IEEE Access*, vol. 12, pp. 55424–55433, 2024.
- [7] B. Zhang, K. Lu, P. Wang, Y. Zhang, B. Zhou, C. Jin, and B. Chi, "Integrated low RCS circularly polarized antenna based on multimode metasurface," *IEEE Antennas Wireless Propag. Lett.*, vol. 24, no. 2, pp. 394–397, Feb. 2025, doi: 10.1109/LAWP.2024.3500029.
- [8] H. L. Yang et al., "Wideband circularly polarized filtering metasurface antenna using split ring resonators and parasitic patches," *IEEE Trans. Antennas Propag.*, early access, 2025.

- [9] Q. Pang, J. Ouyang, F. Yang, S. Yang, and J. Hu, "Inverse design method of antenna based on generative artificial intelligence," *IEEE Antennas Wireless Propag. Lett.*, early access, 2025, doi: 10.1109/LAWP.2025.3562934.